Available online at www.sciencedirect.com
ScienceDirect
Journal of the European Ceramic Society 30 (2010) 319–323
www.elsevier.com/locate/jeurceramsoc

Dependence of dielectric properties on structural characteristics of $(Zn_{1/3}A_{2/3})_{0.5}$ $(Ti_{1-x}B_x)_{0.5}O_2$ ($A = Nb^{5+}$, Ta^{5+}, $B = Ge^{4+}$, Sn^{4+}) ceramics at microwave frequencies

Eung Soo Kim, Seock No Seo *

Department of Materials Engineering, Kyonggi University, Suwon 443-760, Republic of Korea

Available online 10 July 2009

Abstract

The effects of structural characteristics on the dielectric properties of $(Zn_{1/3}A_{2/3})_{0.5}(Ti_{1-x}B_x)_{0.5}O_2$ ($A = Nb^{5+}$, Ta^{5+}, $B = Ge^{4+}$, Sn^{4+}) ($0.1 \leq x \leq 0.3$) ceramics were investigated at microwave frequency. The sintered specimens showed solid solutions with a tetragonal rutile structure within the solid solution range of compositions. With an increase of BO_2, the temperature coefficient of resonant frequency (*TCF*) and dielectric constant (*K*) decreased with a decrease of oxygen octahedral distortion and dielectric polarizabilites, respectively. However, the quality factor (*Qf*) of the sintered specimens was increased with BO_2 due to the reduction of Ti^{4+} ions. The *Qf* value of the specimens with A = Ta was higher than that of the specimens with A = Nb.

Keywords: Rutile structure; Dielectric properties; Octahedral distortion; Sintering

1. Introduction

Various types of dielectric materials have been investigated with efforts to meet the requirements of electronic components for applications of microwave devices. Much attention in this regard has been focused on controlling the dielectric properties of these materials empirically through the formation of solid solutions and mixed phases with two or more compounds.

In order to effectively search for new microwave dielectric materials, the basic relationships between the microwave dielectric properties and crystal structure of the materials should be investigated because the dielectric properties strongly depend on factors such as the composition of the materials, the chemical nature of constituent ions, the distance between cations and anions and the structural characteristics originating from the bonding type. To understand the effects of crystal structure on the microwave dielectric properties, it is necessary to study these basic relationships for a simple crystal structure, rutile structure where there are only two oxygen octahedra in the unit cell of the crystal structure.

Andrade et al.[1] reported the formation of solid solutions of $(Zn_{1/3}A_{2/3})_{1-x}(Ti_yB_{1-y})_xO_2$ with a rutile structure in which divalent, tetravalent, and pentavalent cations were substituted for Ti^{4+}. The substitution of Ti^{4+} ions of TiO_2 by other ions would affect the crystal structures and the microwave dielectric properties of the specimens. The dielectric constant (*K*) at microwave frequencies was found to be not only affected by the dielectric polarizabilities but also rattling of the center ions of oxygen octahedra. Furthermore, the temperature coefficient of resonant frequency (*TCF*) is closely related with the temperature coefficient of dielectric constant (*TCK*), which depends on the distortion of the oxygen octahedral.[2] Also, the rattling effect and the octahedral distortion are largely dependent on the bond strength and bond length of the composing ions.[3]

The ionic size differences between Zn^{2+} (0.74 Å), Nb^{5+} (0.64 Å), Ta^{5+} (0.64 Å), Sn^{4+} (0.69 Å) and/or Ge^{4+}(0.53 Å) and Ti^{4+} (0.605 Å) are not substantial at the same coordination number (C.N. = 6),[4] and complete solid solutions with a rutile structure could be expected. In this study, the dependence of microwave dielectric properties on the crystal structure of $(Zn_{1/3}A_{2/3})_{0.5}(Ti_{1-x}B_x)_{0.5}O_2$ ($A = Nb^{5+}$, Ta^{5+}, $B = Ge^{4+}$, Sn^{4+}) ($0.1 \leq x \leq 0.3$) ceramics were investigated. Effects of Ti^{4+} reduction on the microwave dielectric properties of specimens incorporating various types of ions are also discussed.

* Corresponding author. Tel.: +82 31 249 9774; fax: +82 31 244 6300.
E-mail address: Sns82@kyonggi.ac.kr (S.N. Seo).

0955-2219/$ – see front matter © 2009 Elsevier Ltd. All rights reserved.
doi:10.1016/j.jeurceramsoc.2009.05.042

2. Experimental

High-purity (99.9%) oxide powders of ZnO, Nb_2O_5, Ta_2O_5, SnO_2, GeO_2 and TiO_2 were used as starting materials. They were weighed according to the compositions of ZnA_2O_6 ($A = Nb^{5+}$, Ta^{5+}) and $Ti_{1-x}B_xO_2$ ($B = Sn^{4+}$, Ge^{4+}, $0 \le x \le 0.3$), and then milled with ZrO_2 balls for 24 h in distilled water. Powders with a composition of ZnA_2O_6 and/or $Ti_{1-x}B_xO_2$ were calcined at 900–1200 °C and/or 1100 °C for 3 h, respectively. These calcined powders were mixed according to the formula of $(Zn_{1/3}A_{2/3})_{0.5}(Ti_{1-x}B_x)_{0.5}O_2$. Mixtures with $B = Ge^{4+}$ and/or Sn^{4+} were calcined at 1150 °C and/or 1200 °C for 3 h, respectively. The calcined powders were milled again with ZrO_2 balls for 24 h in distilled water and then dried. The dried powders were pressed into 10 mm diameter disks at 1500 kg/cm^2 isostatically. These disks were sintered from 1200 °C to 1300 °C for 3 h in air. The heating rate was 5 °C/min and the cooling rate was 1 °C/min down to 900 °C, after which the specimens were furnace cooled to room temperature.

Powder X-ray diffraction analysis (D/Max-3C, Rigaku, Japan) with Cu Kα radiation was used to determine the crystalline phases in the calcined and the sintered specimens. XRD data for a Rietveld analysis were collected over a range of $2\theta = 20-80°$ with a step size of 0.02° and a count time of 2 s. From Rietveld refinements of the X-ray diffraction patterns using the Rietan2000 program,[5] the lattice parameters and unit-cell volume of the sintered specimens were determined. The initial structure model for rutile compounds was taken from the study by Abrahams et al.[6] who characterized the crystal structure of $Zn_{0.15}Nb_{0.3}Ti_{0.55}O_2$, using neutron powder diffraction at room temperature. The polished surface of the sintered specimens was observed using a scanning electron microscope (JEOL JSM-6500F, Japan). The X-ray photoelectron spectroscopy (XPS) spectra were measured using a XPS instrument (ESCA2000, VG Scientific, England). During the measurement, the instrument pressure was maintained at 10^{-9} Torr. The Ti 2p XPS spectra were measured using the Al*Kα* line. The measured binding energy was normalized to the C 1s peak (binding energy of 284.6 eV)[7] of adventitious carbon adsorbed on the sintered specimens by contamination from the vacuum pumping oil. Microwave dielectric properties of the specimens were measured by the post-resonant method[8] at 7–9 GHz for the dielectric constant (*K*) and quality factor (*Qf*), and by the cavity method[9] for the *TCF* in a temperature range of 25–80 °C.

3. Results and discussion

Due to the different sintering behaviors of $(Zn_{1/3}A_{2/3})_{0.5}(Ti_{1-x}B_x)_{0.5}O_2$ ($A = Nb^{5+}$, Ta^{5+}, $B = Ge^{4+}$, Sn^{4+}) ($0 \le x \le 0.3$) according to the types of $A^{5+}$and B^{4+} ions, the optimal sintering temperatures for each composition were determined in order to obtain density higher than 94% of the theoretical density. Specimens of $(Zn_{1/3}Ta_{2/3})_{0.5}(Ti_{1-x}Sn_x)_{0.5}O_2$ were sintered at 1300 °C for 3 h, while the other compositions were sintered at 1200 °C for 3 h in air.

Fig. 1 shows the X-ray diffraction patterns of the $(Zn_{1/3}A_{2/3})_{0.5}(Ti_{1-x}B_x)_{0.5}O_2$ ($A = Nb^{5+}$, Ta^{5+}, $B = Ge^{4+}$, Sn^{4+}) sintered specimens. For the specimens with $A = Ta^{5+}$, complete solid solutions with a tetragonal rutile structure (*$P4_2/mnm$*, No. 136) were detected through the entire ranges of composition ($0 \le x \le 0.3$). However, secondary phases of GeO_2 and $ZnTiNb_2O_8$ were detected for $(Zn_{1/3}Nb_{2/3})_{0.5}(Ti_{1-x}Ge_x)_{0.5}O_2$ (ZNTG, $0.25 \le x \le 0.3$) and $(Zn_{1/3}Nb_{2/3})_{0.5}(Ti_{1-x}Sn_x)_{0.5}O_2$ (ZNTS, $x = 0.3$), along with the rutile phase.

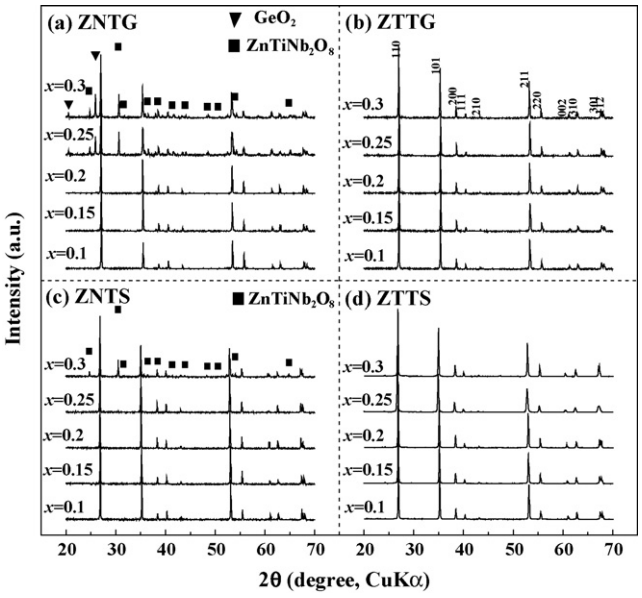

Fig. 1. X-ray diffraction patterns of $(Zn_{1/3}A_{2/3})_{0.5}(Ti_{1-x}B_x)_{0.5}O_2$ sintered specimens. (a) $(Zn_{1/3}Nb_{2/3})_{0.5}(Ti_{1-x}Ge_x)_{0.5}O_2$ (ZNTG), (b) $(Zn_{1/3}Ta_{2/3})_{0.5}(Ti_{1-x}Ge_x)_{0.5}O_2$ (ZTTG), (c) $(Zn_{1/3}Nb_{2/3})_{0.5}(Ti_{1-x}Sn_x)_{0.5}O_2$ (ZNTS) and (d) $(Zn_{1/3}Ta_{2/3})_{0.5}(Ti_{1-x}Sn_x)_{0.5}O_2$ (ZTTS).

Crystallographic data obtained from a Rietveld refinement for $(Zn_{1/3}A_{2/3})_{0.5}(Ti_{1-x}B_x)_{0.5}O_2$ ($A = Nb^{5+}$, Ta^{5+}, $B = Sn^{4+}$, Ge^{4+}) are listed in Table 1. With an increase of GeO_2 content, the unit-cell volume of solid solution deceased, while the unit-cell volume increased with an increase of SnO_2 content. These results could be explained by the difference in the ionic radius of Ge^{4+}(0.53 Å), Ti^{4+}(0.605 Å) and Sn^{4+}(0.69 Å) at the same coordination number (C.N. = 6).[2] The rutile compounds had two apical (d_{apical}) and four equatorial bonds ($d_{equatorial}$) in the oxygen octahedron, which is slightly distorted due to the differences between these bonds[10] depending on the type of center cation of the octahedron. For the specimens with $B = Ge^{4+}$, both bond lengths of the oxygen octahedra decreased with Ge^{4+} content, while the equatorial bonds of the specimens with $B = Sn^{4+}$ increased with the increase of Sn^{4+} content. From the changes of the bond lengths with the type and content of B^{4+} ions, the distortion of the oxygen octahedra could be expected.

There is a close relation between tetragonality (*c*/*a*) and oxygen position parameter (*u*) in the rutile-type structure, which was calculated from the following equation[11]:

$$u = \frac{2 - (4 - 2(1 - (d_{equatorial}/d_{apical})^2)((c/a)^2 + 2))^{1/2}}{4 - (1 - (d_{equatorial}/d_{apical})^2)} \quad (1)$$

If the apical and equatorial bond lengths are equal, that is no octahedral distortion, and the critical value of *u* is obtained ($u_{cry} = \{1/4 + [c^2/(8a^2)]\}$).[12]

Table 1
Crystallographic data and refinement statistics obtained from Rietveld refinement for $(Zn_{1/3}A_{2/3})_{0.5}(Ti_{1-x}B_x)_{0.5}O_2$ (A = Nb^{5+}, Ta^{5+}, B = Sn^{4+}, Ge^{4+}) sintered specimens.

B ion	A ion	x (mol)	Lattice parameters (Å)		$V_{unit\text{-}cell}$ (Å^3)	Bond length (Å)		Ratio of $d_{apical}/d_{equatorial}$	R_{wp} (%)	R_p (%)
			a	c		d_{apical}	$d_{equatorial}$			
Ge^{4+}	Nb^{5+}	0.1	4.7171	3.0503	67.873	2.065	1.985	1.0403	11.50	8.66
		0.15	4.7151	3.0491	67.790	2.040	1.983	1.0287	12.29	8.93
		0.2	4.7123	3.0472	67.665	2.010	1.981	1.0146	10.58	7.65
	Ta^{5+}	0.1	4.6988	3.0455	67.240	2.042	1.970	1.0365	8.30	6.46
		0.15	4.6987	3.0447	67.220	2.027	1.969	1.0295	8.63	6.40
		0.2	4.6987	3.0447	67.219	2.022	1.968	1.0274	9.20	6.95
		0.25	4.6983	3.0447	67.208	2.011	1.967	1.0224	8.39	6.08
		0.3	4.6981	3.0446	67.201	2.001	1.966	1.0178	9.29	7.24
Sn^{4+}	Nb^{5+}	0.1	4.7167	3.0538	67.938	2.068	1.984	1.0423	10.79	8.33
		0.15	4.7178	3.0581	68.066	2.062	1.990	1.0362	10.66	8.17
		0.2	4.7186	3.0623	68.183	2.055	1.996	1.0296	9.71	7.38
		0.25	4.7201	3.0674	68.341	2.053	2.000	1.0265	14.71	10.98
	Ta^{5+}	0.1	4.6919	3.0444	67.020	2.043	1.985	1.0292	7.55	5.78
		0.15	4.6981	3.0517	67.358	2.044	1.990	1.0271	6.92	5.28
		0.2	4.7043	3.0588	67.694	2.042	1.997	1.0225	6.59	4.20
		0.25	4.7095	3.0655	67.992	2.040	2.003	1.0185	5.62	3.55
		0.3	4.7149	3.0741	68.339	2.038	2.011	1.0134	5.66	3.97

Even though the variations of both bond lengths showed different behaviors according to the type of B^{4+} ions (Table 1), the deviation of the oxygen position parameter (u) from the critical value (u_{cry}) decreased with the content of B^{4+} ions, corresponding to a decrease of octahedral distortion, as shown in Table 2. These results are also in agreement with the octahedral distortion (Δ) obtained from the individual bond length of the oxygen octahedron via the following equation[4]:

$$\Delta = \frac{1}{6}\sum\left\{\frac{R_i - \bar{R}}{R}\right\}^2 \quad (2)$$

Table 2
Octahedral distortion and TCF of $(Zn_{1/3}A_{2/3})_{0.5}(Ti_{1-x}B_x)_{0.5}O_2$ (A = Nb^{5+}, Ta^{5+}, B = Sn^{4+}, Ge^{4+}) sintered specimens.

B ion	A ion	x (mol)	u	u–u_{cry}	Distortion ($\Delta \times 10^5$)	TCF (ppm/°C)
Ge^{4+}	Nb^{5+}	0.1	0.310	0.0073	35.14	112.5
		0.15	0.307	0.0052	18.01	104.5
		0.2	0.305	0.0027	4.72	94.2
	Ta^{5+}	0.1	0.309	0.0066	28.97	81.6
		0.15	0.308	0.0053	18.91	79.3
		0.2	0.307	0.0050	16.43	71.9
		0.25	0.307	0.0041	10.96	71.9
		0.3	0.306	0.0032	6.96	63.9
Sn^{4+}	Nb^{5+}	0.1	0.310	0.0077	38.73	112.1
		0.15	0.309	0.0066	28.40	73.0
		0.2	0.308	0.0054	19.04	48.9
		0.25	0.308	0.0048	15.33	43.2
	Ta^{5+}	0.1	0.308	0.0053	18.61	85.9
		0.15	0.308	0.0049	16.07	61.4
		0.2	0.307	0.0041	11.12	35.4
		0.25	0.306	0.0034	7.49	24.7
		0.3	0.306	0.0025	3.97	15.3

where R_i is the individual bond length and $\bar{R}$ is the average bond length of the oxygen octahedron.

The TCF was affected by structural characteristics of the oxygen octahedral distortion.[13] TCF of

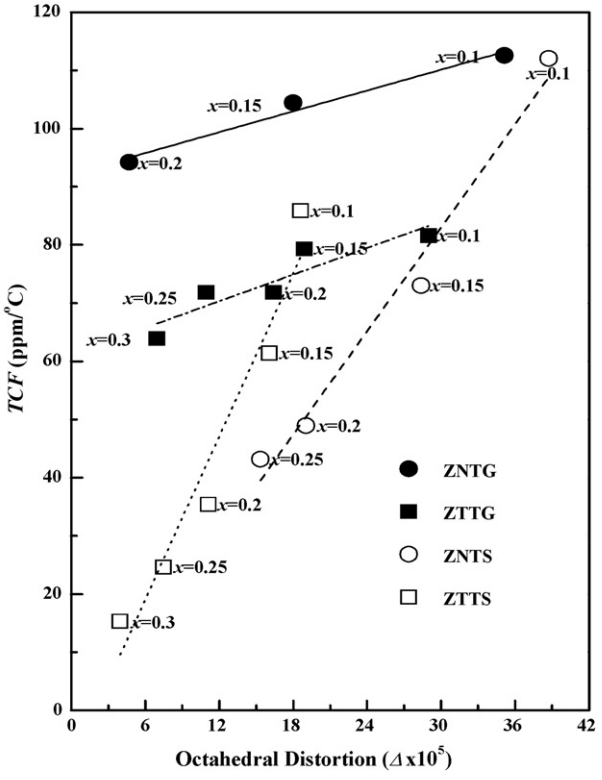

Fig. 2. Dependence of TCF on octahedral distortion of $(Zn_{1/3}A_{2/3})_{0.5}(Ti_{1-x}B_x)_{0.5}O_2$ sintered specimens. $(Zn_{1/3}Nb_{2/3})_{0.5}(Ti_{1-x}Ge_x)_{0.5}O_2$ (ZNTG), $(Zn_{1/3}Ta_{2/3})_{0.5}(Ti_{1-x}Ge_x)_{0.5}O_2$ (ZTTG), $(Zn_{1/3}Nb_{2/3})_{0.5}(Ti_{1-x}Sn_x)_{0.5}O_2$ (ZNTS) and $(Zn_{1/3}Ta_{2/3})_{0.5}(Ti_{1-x}Sn_x)_{0.5}O_2$ (ZTTS).

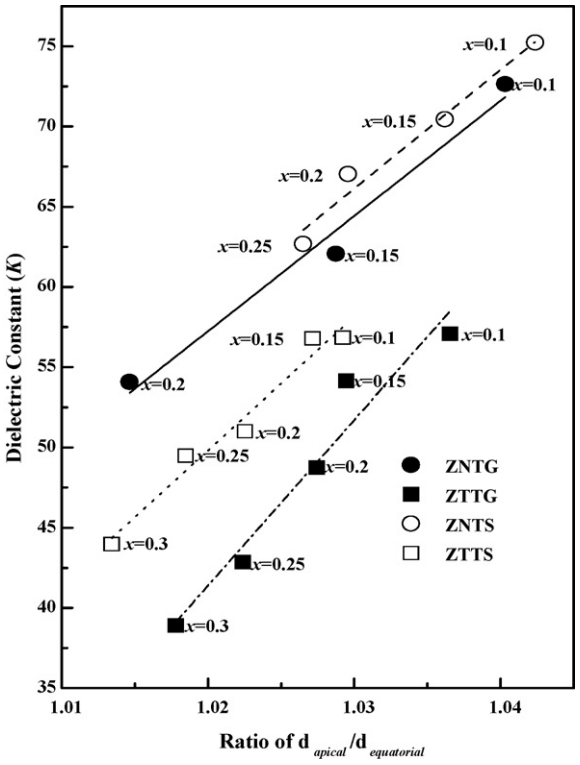

Fig. 3. Dependence of dielectric constant (K) on ratio of $d_{apical}/d_{equatorial}$ of $(Zn_{1/3}A_{2/3})_{0.5}(Ti_{1-x}B_x)_{0.5}O_2$ sintered specimens. $(Zn_{1/3}Nb_{2/3})_{0.5}$-$(Ti_{1-x}Ge_x)_{0.5}O_2$ (ZNTG), $(Zn_{1/3}Ta_{2/3})_{0.5}(Ti_{1-x}Ge_x)_{0.5}O_2$ (ZTTG), $(Zn_{1/3}Nb_{2/3})_{0.5}(Ti_{1-x}Sn_x)_{0.5}O_2$ (ZNTS) and $(Zn_{1/3}Ta_{2/3})_{0.5}(Ti_{1-x}Sn_x)_{0.5}O_2$ (ZTTS).

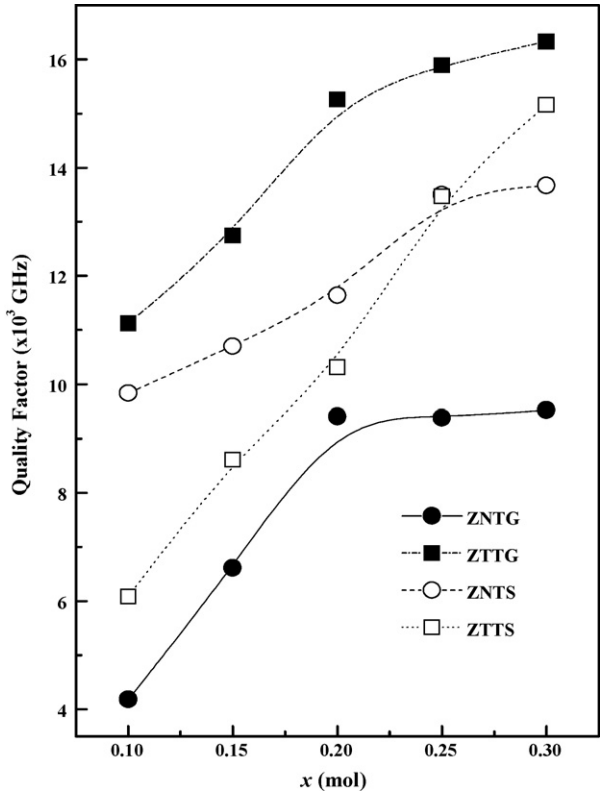

Fig. 4. Quality factor (Qf) of $(Zn_{1/3}A_{2/3})_{0.5}(Ti_{1-x}B_x)_{0.5}O_2$ sintered specimens. $(Zn_{1/3}Nb_{2/3})_{0.5}(Ti_{1-x}Ge_x)_{0.5}O_2$ (ZNTG), $(Zn_{1/3}Ta_{2/3})_{0.5}(Ti_{1-x}Ge_x)_{0.5}O_2$ (ZTTG), $(Zn_{1/3}Nb_{2/3})_{0.5}(Ti_{1-x}Sn_x)_{0.5}O_2$ (ZNTS) and $(Zn_{1/3}Ta_{2/3})_{0.5}$-$(Ti_{1-x}Sn_x)_{0.5}O_2$ (ZTTS).

$(Zn_{1/3}A_{2/3})_{0.5}(Ti_{1-x}B_x)_{0.5}O_2$ ($A = Nb^{5+}$, Ta^{5+}, $B = Sn^{4+}$, Ge^{4+}) ceramics linearly decreased with a decrease of octahedral distortion, as shown in Fig. 2. Therefore, the large positive value of TCF in the TiO_2 rutile structure could be controlled by substitution of tetravalent Sn^{4+} and Ge^{4+}.

Dielectric constants (K) of $(Zn_{1/3}A_{2/3})_{0.5}(Ti_{1-x}B_x)_{0.5}O_2$ ($A = Nb^{5+}$, Ta^{5+}, $B = Ge^{4+}$, Sn^{4+}) ceramics decreased with GeO_2 and SnO_2 content, because the dielectric polarizabilities of GeO_2 (5.65 Å^3) and SnO_2 (6.85 Å^3) were smaller than that of TiO_2 (6.95 Å^3).[14]

For the solid solutions of $(Zn_{1/3}A_{2/3})_{0.5}(Ti_{1-x}B_x)_{0.5}O_2$ ($A = Nb^{5+}$, Ta^{5+}, $B = Ge^{4+}$, Sn^{4+}), K of the specimens with $A = Nb^{5+}$ (ZNTB) was larger than that of the specimens with $A = Ta^{5+}$ (ZTTB) at the same BO_2 ($B = Ge^{4+}$, Sn^{4+}) content, even though the dielectric polarizabilities of $ZnTa_2O_6$ (23.56 Å^3) were larger than that of $ZnNb_2O_6$ (22.04 Å^3). This could be explained by the structural characteristics of the rutile structure. As confirmed in Table 1, the bond length ratios ($d_{apical}/d_{equatorial}$) of ZNTB were larger than those of ZTTB. In comparison with ZTTB, the higher K of ZNTB resulted from the larger apical extension, which leads to an increase of rattling space by the apical direction within the oxygen octahedron. In addition, the bond length ratio ($d_{apical}/d_{equatorial}$) decreased with BO_2 ($B = Ge^{4+}$, Sn^{4+}) content, and the dielectric constants (K) of the specimens then decreased with a decrease of $d_{apical}/d_{equatorial}$, as shown in Fig. 3.

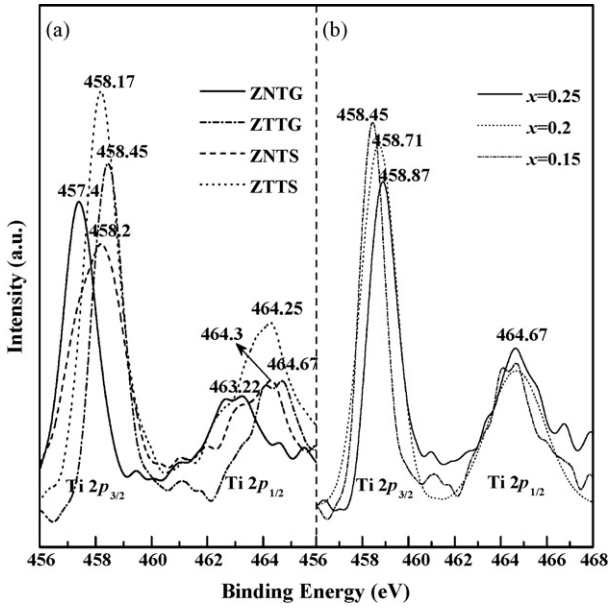

Fig. 5. X-ray photoelectron spectra (XPS) of (a) Ti 2p for $(Zn_{1/3}A_{2/3})_{0.5}$ $(Ti_{0.85}B_{0.15})_{0.5}O_2$ ($A = Nb^{5+}$, Ta^{5+}, $B = Sn^{4+}$, Ge^{4+}) and (b) $(Zn_{1/3}Ta_{2/3})_{0.5}(Ti_{1-x}Ge_x)_{0.5}O_2$ ($x = 0.15$, 0.2 and 0.25) sintered specimens.

Fig. 4 shows the *Qf* of the $(Zn_{1/3}A_{2/3})_{0.5}(Ti_{1-x}B_x)_{0.5}O_2$ ($A = Nb^{5+}, Ta^{5+}$, $B = Sn^{4+}, Ge^{4+}$) specimens. *Qf* values increased with SnO_2 and/or GeO_2 content, while those of specimens with $A = Nb^{5+}$ did not increase above $x = 0.20$ for $B = Ge^{4+}$ and $x = 0.25$ for $B = Sn^{4+}$, respectively, due to the formation of secondary phases of GeO_2 and $ZnTiNb_2O_8$, as confirmed in Fig. 1. For the sintered specimens of $(Zn_{1/3}A_{2/3})_{0.5}(Ti_{0.9}\ B_{0.1})_{0.5}O_2$ ($A = Nb^{5+}$, Ta^{5+}, $B = Sn^{4+}$, Ge^{4+}) ($x = 0.1$), dark gray color appeared inside the specimens. With further substitution of BO_2, the color gradually changed to bright yellow. This was related to a reduction of Ti^{4+} ions, observed in titanium-containing ceramics, due to the small amount of Ti^{3+} and oxygen vacancies formed during processing.[15] To confirm the reduction of Ti^{4+} ions, X-ray photoelectron spectra (XPS) of $(Zn_{1/3}A_{2/3})_{0.5}(Ti_{0.85}B_{0.15})_{0.5}O_2$ ($A^{5+} = Nb, Ta$, $B^{4+} = Ge, Sn$) ceramics are shown in Fig. 5. The high *Qf* value of the specimens reflects high binding energy of Ti 2p peaks, because the binding energy decreased with a reduction of Ti ions. In addition, the binding energy of the Ti 2p peaks of $(Zn_{1/3}Ta_{2/3})_{0.5}(Ti_{1-x}Ge_x)_{0.5}O_2$ increased with GeO_2 content. For the system of $(Zn_{1/3}A_{2/3})_{0.5}(Ti_{1-x}B_x)_{0.5}O_2$ ($A^{5+} = Nb, Ta$, $B^{4+} = Ge, Sn$), the *Qf* values are strongly dependent on the reduction of Ti ions, which resulted from substitution ions of A- and B-site of $(Zn_{1/3}A_{2/3})_{0.5}(Ti_{1-x}B_x)_{0.5}O_2$ ceramics.

4. Conclusion

The dependence of microwave dielectric properties on the structural characteristics of $(Zn_{1/3}A_{2/3})_{0.5}(Ti_{1-x}B_x)_{0.5}O_2$ ($A = Nb^{5+}$, Ta^{5+}, $B = Ge^{4+}$, Sn^{4+}) ($0.1 \le x \le 0.3$) was investigated. The sintered specimens showed a tetragonal rutile structure through a solid solution range of composition and secondary phases of GeO_2 and/or $ZnTiNb_2O_8$ were detected with $(Zn_{1/3}Nb_{2/3})_{0.5}(Ti_{1-x}B_x)_{0.5}O_2$ ($B = Ge^{4+}$, Sn^{4+}) ($0.25 \le x \le 0.3$ for $B = Ge^{4+}$ and/or $x = 0.3$ for $B = Sn^{4+}$). For the solid solution range, the *TCF* decreased with a decrease of oxygen octahedral distortion. The dielectric constant (K) of the sintered specimens decreased with an increase of BO_2 content due to a decrease of bond length ratio of $(d_{apical})/(d_{equatorial})$ and dielectric polarizabilities. Furthermore, the quality factor of the sintered specimens increased with BO_2 content, due to decreased reduction of Ti^{4+} ions.

Acknowledgements

This work was supported by a Korea Research Foundation Grant funded by the Korean Government (MOEHRD; KRF-2006-311-D00527).

References

[1]. Andrade, J., Villafuerte-Castrejon, M. E., Valenzuela, R. and West, A. R., Rutile solid solutions containing M^+(Li), M^{2+}(Zn, Mg), M^{3+}(Al) and M^{5+} (Nb, Ta, Sb) ions. *J. Mater. Sci. Lett.*, 1986, **5**, 147–149.

[2]. Reany, I. M., Colla, E. L. and Setter, N., Dielectric and structural characteristics of Ba- and Sr-based complex perovskites as a function of tolerance factor. *Jpn. J. Appl. Phys.*, 1994, **33**, 3984–3990.

[3]. Kim, E. S., Chun, B. S. and Yoon, K. H., Dielectric properties of $[Ca_{1-x}(Li_{1/2}Nd_{1/2})_x]_{1-y}Zn_yTiO_3$ ceramics at microwave frequencies. *Mater. Sci. Eng.*, 2003, **B99**, 93–97.

[4]. Shannon, R. D., Revised effective ionic radii and systematic studies of interatomic distances in halides and chalcogenides. *Acta Cryst.*, 1976, **A32**, 751–767.

[5]. Izumi, F. and Ikeda, T., A Rietveld-analysis program RIETAN-98 and its applications to zeolites. *Mater. Sci. Forum*, 2000, **321–324**, 198–203.

[6]. Abrahams, I., Bruce, P. G., David, W. I. F. and West, A. R., Structure determination of substituted rutiles by time-of-flight neutron diffraction. *Chem. Mater.*, 1989, **1**, 237–240.

[7]. Estrade-Szwarckopf, H. and Rousseau, B., Photoelectron core level spectroscopy study of Cs–graphite intercalation compounds. I. Clean surfaces study. *J. Phys. Chem. Solids*, 1992, **53**, 419.

[8]. Hakki, B. W. and Coleman, P. D., A dielectric resonator method of measuring inductive capacities in the millimeter range. *IRE Trans. Microwave Theory Technol.*, 1960, **8**, 402–410.

[9]. Nishikawa, T., Wakino, K., Tamura, H., Tanaka, H. and Ishikawa, Y., Precise measurement method for temperature coefficient of microwave dielectric resonator material. *IEEE MTT-S Int. Microwave Symp. Dig.*, 1987, **87**, 277–280.

[10]. Mo, S. D. and Ching, W. Y., Electronic and optical properties of three phases of titanium dioxide: rutile, anatase, and brookite. *Phys. Rev.*, 1995, **B51**, 13023–13032.

[11]. Ji-Won Choiw, R. B. and van Dover, Correlation between temperature coefficient of resonant frequency and tetragonality ratio. *J. Am. Ceram. Soc.*, 2006, **89**, 1144–1146.

[12]. Hirata, T., Oxygen position, octahedral distortion, and bond-valence parameter from bond lengths in $Ti_{1-x}Sn_xO_2$ ($0 \le x \le 1$). *J. Am. Ceram. Soc.*, 2000, **83**, 3205–3207.

[13]. Colla, E. L., Reaney, I. M. and Setter, N., Effect of structural changes in complex perovskites on temperature coefficient of the relative permittivity. *J. Appl. Phys.*, 1993, **74**, 3414–3425.

[14]. Shannon, R. D., Dielectric polarizabilities of ions in oxides and fluorides. *J. Appl. Phys.*, 1993, **73**, 348–366.

[15]. Michiura, N., Tatekawa, T., Higuchi, Y. and Tamura, H., Role of donor and acceptor ions in the dielectric loss tangent of $(Zn_{0.8}Sn_{0.2})TiO_4$ dielectric resonator material. *J. Am. Ceram. Soc.*, 1995, **78**, 793–796.